We are IntechOpen, the world's leading publisher of Open Access books
Built by scientists, for scientists

6,900
Open access books available

185,000
International authors and editors

200M
Downloads

154
Countries delivered to

Our authors are among the

TOP 1%
most cited scientists

12.2%
Contributors from top 500 universities

CLARIVATE ANALYTICS
BOOK CITATION INDEX
INDEXED

WEB OF SCIENCE™

Selection of our books indexed in the Book Citation Index
in Web of Science™ Core Collection (BKCI)

Interested in publishing with us?
Contact book.department@intechopen.com

Numbers displayed above are based on latest data collected.
For more information visit www.intechopen.com

Chapter

Effect of Operating Parameters and Foreign Ions on the Crystal Growth of Calcium Carbonate during Scale Formation: An Overview

Atef Korchef

Abstract

Due to the insufficiency of freshwater resources and to supply the drinking water populations, many desalination processes such as reverse osmosis, electrodialysis and distillation are widely used. However, these processes are of large-scale consumers of energy and confronted with various problems such as corrosion and scale formation. In most cases, scales are made of calcium carbonate $CaCO_3$. In the present chapter, an overview on the effect of operating parameters such as temperature, pH and supersaturation on the precipitation kinetics, microstructure, and polymorphism of $CaCO_3$ is given. Additionally, I put special emphasis on the effect of foreign ions such as magnesium, sulphate, and iron ions on $CaCO_3$ precipitation since they are present at significant concentrations in natural waters. Also, the mechanisms by which these ions affect the crystal growth of $CaCO_3$ were pointed out. Knowledge about these operating parameters as well as the effects of foreign ions allow elucidating the polymorphs growth during water treatment. The control of these operating parameters allows reducing scale formation during drinking water and wastewater treatment. The economic impact is of greatest importance since this favorably affects the treatment costs, increases the equipment life, and allows enhanced product water recovery.

Keywords: water treatment, scale, calcium carbonate, cement, growth, magnesium, sulphate, iron, CO_2, supersaturation, pH, temperature

1. Introduction

Calcium carbonate $CaCO_3$ is a commercial material and a major constituent in many natural systems. $CaCO_3$ is widespread in the natural environment such as eggshells, corals, and sedimentary rocks [1–3]. $CaCO_3$ is applied as filler and pigment in the production of paper, rubber, plastic, paint, textiles, and pharmaceuticals [4, 5]. More interesting, $CaCO_3$ is used in ionic cements which are widely used in bone and dental replacement biomaterials. Original compositions of bioresorbable and biocompatible cements including a significant proportion of synthetic $CaCO_3$ have been developed to meet a need for biomedical cements with

increased resorption properties. Bone substitutes based on chemically treated natural $CaCO_3$ are biocompatible and bioactive. They are used in the form of powder and porous ceramics [6–11]. Because of the higher solubility of calcium carbonates compared to calcium phosphates, the introduction of a significant amount of a metastable variety of $CaCO_3$ (vaterite or aragonite) should give mineral cements a higher rate of resorption and thus promote faster bone reconstruction [11, 12].

On the other hand, $CaCO_3$ has a significant impact on energy production and water treatment. The insufficiency of the freshwater resources and the requirements of drinking water will be increasingly manifest in the years to come. It is very probable that the problem of water, just like that of the energy resources, will be regarded as one of the determining factors of the stability of a country. The surest and economic means to supply the drinking water populations require the desalination of brackish, saline or sea waters by using different processes of desalination (reverse osmosis, electrodialysis, distillation, etc). However, these processes are generally of large-scale consumers of energy and confronted with various problems, such as corrosion and scale formation (**Figure 1**) which cause enormous energy losses. In most cases, scales are made of the sparingly soluble salt $CaCO_3$ [13–19]. Because of its poor thermal conductivity and its good adherence to the walls, $CaCO_3$ decreases the heat transfer rate, reduces the water flow rate, and even shortens equipment life by corrosion [20, 21]. The crystallization of $CaCO_3$ depends on several operating parameters such as the mineralogical water composition, the supersaturation of the treated water, the pH, and the temperature.

In the present overview chapter, I was interested in the scale problem through $CaCO_3$ precipitation encountered during drinking water and wastewater treatment plants. The effect of the operating parameters such as temperature, pH, supersaturation, and foreign ions on the $CaCO_3$ crystal growth, microstructure and polymorphism was exposed. Knowledge about these operating parameters for $CaCO_3$ crystallization as well as the effects of foreign ions, especially magnesium, sulphate, and iron ions, is very important in the elucidation of the $CaCO_3$ polymorphs growth during water treatment. The presence of mineral ions can have a major influence on the crystal growth and microstructure of $CaCO_3$ since they are present with significant concentrations in natural waters. The economic impact is of the utmost importance. Indeed, the control of the operating parameters makes it possible to inhibit or reduce the scale formation during the treatment of drinking water and wastewater in different industrial processes such as desalination units, water pumps

Figure 1.
Scaling through $CaCO_3$ precipitation in drinking water pipes.

and heat exchangers. This positively affects processing costs, increases the life of the equipment, and enhances the product water recovery.

2. Polymorphism of calcium carbonate

Calcium carbonate has six different polymorphs: one amorphous $CaCO_3$, two hydrated crystalline ones (hexahydrate $CaCO_3 \cdot 6H_2O$ and monohydrate $CaCO_3 \cdot H_2O$), and three anhydrous crystalline polymorphs that are the hexagonal vaterite, the orthorhombic aragonite and the rhombohedra calcite [22–25]. The X-ray diffraction (XRD) diagrams of these polymorphs are shown in **Figure 2**. For $CaCO_3$ polymorphs, the solubility increases in the order of calcite, aragonite, and vaterite [26, 27]. Calcite is the most stable polymorph under ambient atmospheric conditions [26]. In the presence of water, vaterite, which is the least thermodynamically stable polymorph, easily transforms into the more stable calcite or aragonite [28]. Environmental conditions play effective roles in crystal growth and morphological changes, namely, the solution supersaturation, calcium concentration, pH, and temperature. These experimental parameters should operate together and control the polymorphism of $CaCO_3$.

3. System $CaCO_3$-H_2O-CO_2

Scaling is a complex phenomenon that takes a long time to manifest itself in industrial or domestic facilities. Several techniques, such as mechanical stirring [29], aeration [30], electrochemical precipitation [31], magnetic water treatment [32] have been used in laboratories to assess the effectiveness of chemical or physical treatment, and the influence of certain parameters on scale formation over time. However, the most interesting method used for $CaCO_3$ precipitation is the CO_2 repelling method [16, 17, 33] where the CO_2 containing solution is air bubbled which increases the solution pH and provokes the $CaCO_3$ precipitation (**Figure 3**). Indeed, this method is an accelerated simulation of the natural scaling phenomenon
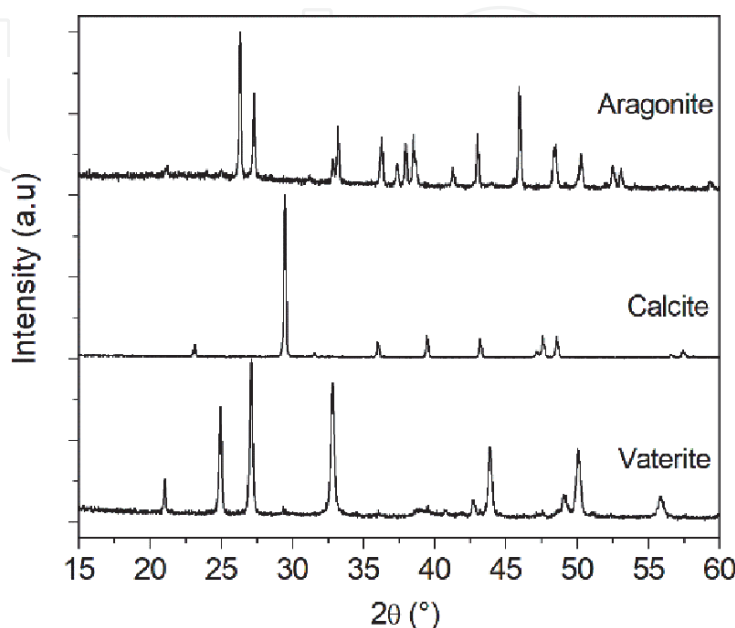

Figure 2.
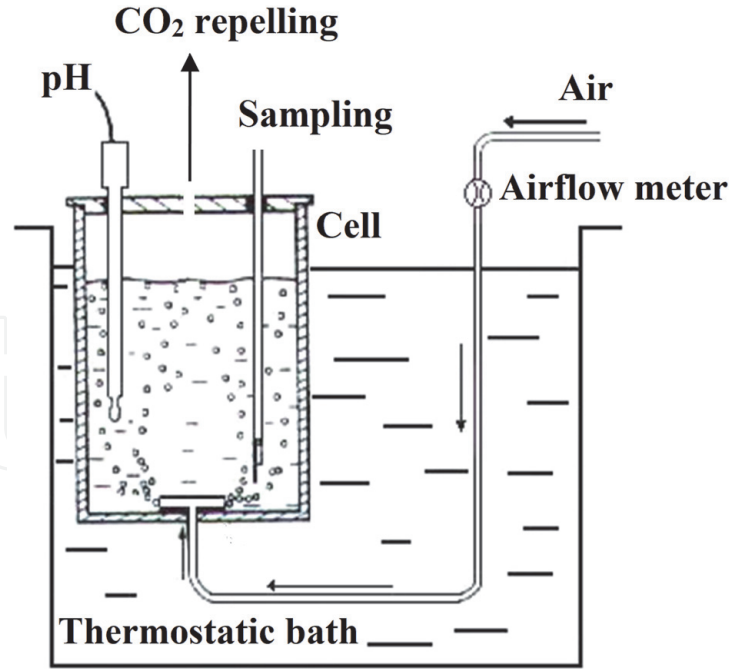*XRD diagrams of vaterite, calcite and aragonite.*

Figure 3.
Schematic illustration of the CO₂ repelling method used for CaCO₃ precipitation. A cylindrical cell containing a diffuser at the bottom and covered with a lid. The lid contains different openings, one of which allows samples to be removed to determine the calcium amount left in the solution and another opening allows CO₂ repelling from the solution while the air is bubbling. The flow of the injected air was controlled by an air flow meter, and the temperature of the solution was controlled by a thermostat with circulating water. An electrode is used to record the pH.

in which the precipitation of CaCO₃ takes place, in a short experiment time that do not exceed 90 min, following the removal of the dissolved CO₂ by the atmospheric air, according to the following reaction [16, 17]:

$$Ca^{2+} + 2HCO_3^- \rightarrow CaCO_3 + CO_2 + H_2O \qquad (1)$$

The saturation index (SI) is a measure of the deviation of the system from equilibrium. When SI < 0, the solution is undersaturated and no crystallization occurs. When SI = 0, the solution is in equilibrium, and when SI > 0, the solution is supersaturated, and crystallization could occur spontaneously. For CaCO₃, SI is given by the following equation:

$$SI = log\,\Omega \qquad (2)$$

where $\Omega = \frac{IAP}{K_{sp}} = \frac{(Ca^{2+})(CO_3^{2-})}{K_{sp}}$ is the supersaturation ratio of the solution with respect to CaCO₃ and IAP and K_{sp} represent respectively, the ionic activity product and the thermodynamic solubility product of CaCO₃. The solubility products of the different polymorphs of CaCO₃, given in **Table 1**, were determined by the temperature dependent equations given by Plummer and Busenberg [27] and Brecevic and Kralj [4]. $(Ca^{2+}) = \gamma_{Ca^{2+}}[Ca^{2+}]$ and $(CO_3^{2-}) = \gamma_{CO_3^{2-}}[CO_3^{2-}]$ are the activities of the ions Ca²⁺ and CO₃²⁻, respectively. The activity coefficients $\gamma_{Ca^{2+}}$ and $\gamma_{CO_3^{2-}}$ are calculated using the extended Debye-Huckel equation:

$$log\,\gamma_i = -\frac{AZ_i^2\sqrt{I}}{1 + Ba_i\sqrt{I}} + b_i\sqrt{I} \qquad (3)$$

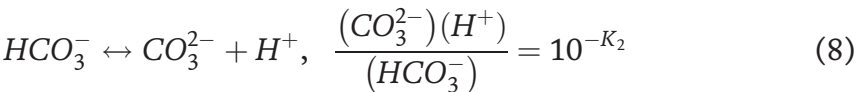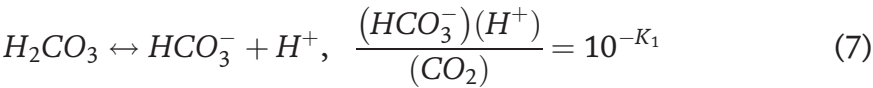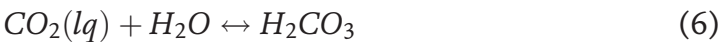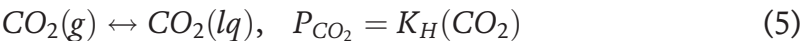| Polymorphs	−log Ks	T in the range	Ref.
Calcite	$171.9065 + 0.077993\,T - 2839.319/T - 71.595\log(T)$, T in K	0–90°C	[27]
Vaterite	$172.1295 + 0.077996\,T - 3074.688/T - 71.595\log(T)$, T in K	0–90°C	[27]
Aragonite	$171.9773 + 0.077993\,T - 2903.293/T - 71.595\log(T)$, T in K	0–90°C	[27]
Amorphous	$6.1987 + 0.0053369\,T + 0.000109\,T^2$, T in °C	10–55°C	[4]
$CaCO_3 \cdot H_2O$	$7.050 + 0.000159\,T^2$, T in °C	10–50°C	[4]
$CaCO_3 \cdot 6H_2O$	$7.1199 + 0.011756\,T + 0.000075556\,T^2$, T in °C	10–25°C	[4]

Table 1.
Logarithmic solubility products of the various polymorphs of calcium carbonate $CaCO_3$ as a function of temperature.

where A, B are constants defined by Harmer [34], a_i and b_i are ion-specific parameters assigned by Truesdell and Jones [35], Z_i is the valence of the i-species and I is the ionic strength:

$$I = \frac{1}{2}\sum_i Z_i^2 c_i \qquad (4)$$

where c_i is the concentration of the i-species.

In the carbonation process, the CO_2 gas firstly dissolves into water to form the carbonic acid H_2CO_3 which transforms into HCO_3^-, CO_3^{2-} and H^+ according to the following equations:

$$CO_2(g) \leftrightarrow CO_2(lq), \quad P_{CO_2} = K_H(CO_2) \qquad (5)$$

$$CO_2(lq) + H_2O \leftrightarrow H_2CO_3 \qquad (6)$$

$$H_2CO_3 \leftrightarrow HCO_3^- + H^+, \quad \frac{(HCO_3^-)(H^+)}{(CO_2)} = 10^{-K_1} \qquad (7)$$

$$HCO_3^- \leftrightarrow CO_3^{2-} + H^+, \quad \frac{(CO_3^{2-})(H^+)}{(HCO_3^-)} = 10^{-K_2} \qquad (8)$$

where K_H, K_1 and K_2 are the Henry's law coefficient, first and second dissociation constants of carbonic acid (given in **Table 2** [36]), respectively and (HCO_3^-), (H^+) and (CO_2) are the activities of the ions HCO_3^-, H^+ and CO_2, respectively.

The electric neutrality of the calco-carbonic solution gives:

$$2[Ca^{2+}] + [H^+] = [OH^-] + [HCO_3^-] + 2[CO_3^{2-}] \qquad (9)$$

and

$$(CO_3^{2-}) = \gamma_{CO_3^{2-}}[CO_3^{2-}] = \frac{1}{2}\gamma_{CO_3^{2-}}(2[Ca^{2+}] + [H^+] - [OH^-] - [HCO_3^-]) \qquad (10)$$

From Eq. (8), the activity of CO_3^{2-} is determined by:

$$(CO_3^{2-}) = (HCO_3^-)10^{pH-K_2} = \gamma_{HCO_3^-}[HCO_3^-]10^{pH-K_2} \qquad (11)$$

where $\gamma_{CO_3^{2-}}$ and $\gamma_{HCO_3^-}$ are the activities coefficients of the ions CO_3^{2-} and HCO_3^-, respectively. It is worth to note that the concentration of HCO_3^- ions can be assumed to be equal to the total alkali concentration (TAC) for pH in the range

Carbonation process	CO_2 (g) $\leftrightarrow$ CO_2 (lq)	CO_2 (lq) + H_2O $\leftrightarrow$ H_2CO_3 H_2CO_3 $\leftrightarrow$ HCO_3^- + H^+	HCO_3^- $\leftrightarrow$ CO_3^{2-} + H^+
Equilibrium equation	$P_{CO_2} = K_H(CO_2)$	$\frac{(HCO_3^-)(H^+)}{(CO_2)} = 10^{-K_1}$	$\frac{(CO_3^{2-})(H^+)}{(HCO_3^-)} = 10^{-K_2}$
Equilibrium constants	$K_H \times 10^{-5}$ (PaLmol^{-1})	K_1	K_2
Temperature (°C) 25	22.549	6.4	10.35
30	33.769	6.37	10.31
40	42.586	6.34	10.24
50	51.920	6.32	10.19
60	61.476	6.33	10.16

Table 2.
Henry's law coefficient (K_H), and first and second dissociation constants (K_1, K_2) of carbonic acid for different temperatures (values are taken from Ref. [36]).

6–8.8. Indeed, $[CO_3^{2-}]$ and $[OH^-]$ are small in this pH range [37] and in a first approximation:

$$TAC = [HCO_3^-] + 2[CO_3^{2-}] + [OH^-] \approx [HCO_3^-] \tag{12}$$

4. Effect of operating parameters on CaCO$_3$ precipitation

The solubility of $CaCO_3$ polymorphs increases in the order of calcite, aragonite, and vaterite [26, 27]. Environmental conditions play effective roles in the crystal growth and morphological changes of $CaCO_3$. Indeed, the nucleation and growth kinetics of $CaCO_3$ as well as the morphology and polymorphism of the obtained precipitates are affected by various key operating parameters such as supersaturation [23, 28, 38], temperature [37, 39, 40], and pH [41–43]. These experimental parameters operate together and control the polymorphism of $CaCO_3$. For example, it was shown that vaterite can be obtained at high superasaturations and low calcium concentrations typically below 10^{-2} M [44], solution pH in the range 8.5–10 [45] and/or low temperatures in the range 20–40°C [45, 46].

Söhnel and Mullin [38] showed that the crystal growth rate of $CaCO_3$ increased with increasing the solution supersaturation. Vaterite was favored in moderate (S < 6.5) to enhanced supersaturation solutions [28, 44] and smaller vaterite crystals were obtained when supersaturation increased [28]. High supersaturations in the range 4−14 prevented the transformation of vaterite into calcite and increased the crystal growth rate [16, 23].

It is worth noticing that the initial calcium concentration in the solution has an important impact on the polymorphism of $CaCO_3$. Indeed, it was found that calcite did not crystallize at decreased Ca^{2+} concentrations (typically below 10^{-2} M), and only vaterite was obtained when $CaCO_3$ was prepared, at 25°C, by a CO_2/N_2 mixed gas bubbled into a solution of $CaCO_3$ [23]. This agrees with the results of Korchef [16] who showed that vaterite was the predominant polymorph at 28°C, for a supersaturation in the range 4–14, and calcite was not detected, because of the low initial calcium concentration (4×10^{-3} M). Thus, for a solution supersaturated with respect to calcite (~15–62), aragonite (4–17) and vaterite (10–38), vaterite was favored for an initial calcium concentration 4×10^{-3} M ($<10^{-2}$ M), a precipitation pH in the range 8.4–8.8 and a temperature of 28°C [16].

The temperature and the solution pH are considered as critical parameters in controlling the kinetics crystallization, polymorphism, and morphology of $CaCO_3$ particles. At room temperature, calcite is the most predominant phase. At temperatures higher than 50°C, $CaCO_3$ precipitates as needles-like aragonite crystals [47–50]. At conditions of spontaneous $CaCO_3$ formation preceded by the lapse of induction time, the increase of temperature, at fixed ionic strength, results to the decrease of the induction time and to the increase of the crystalline growth rate and also the amount precipitated [37]. Chen and Xiang [46] investigated the effect of temperature on the structures and morphology of $CaCO_3$ crystals obtained by double injection of $CaCl_2$ and NH_4HCO_3 solutions with a 1:1 molar ratio. At 30−40°C, they obtained crystals of lamellar vaterite. At higher temperatures of 50–70°C, a mixture of calcite and aragonite formed, and only aragonite whiskers crystallized at a temperature of 80°C. However, aragonite was not detected when $CaCO_3$ precipitated by mixing calcium acetate $Ca(C_2H_3O_2)_2$ and ammonium carbonate $(NH_4)_2CO_3$ [40].

In their recent publication, Korchef and Touabi [17] studied the effect of temperature and initial solution pH on the crystallization of $CaCO_3$ by CO_2 repelling. They showed that vaterite and aragonite were the polymorphs of $CaCO_3$ collected at 28°C and 50°C and the increase in temperature from 28–50°C leads to the acceleration of $CaCO_3$ nucleation and crystal growth. This is was explained by higher supersaturations with respect to aragonite (in the range $\sim$ 40–69) and vaterite (between $\sim$12 and 21) obtained at 50°C than those obtained at 28°C. The increase of the initial solution pH accelerates the $CaCO_3$ precipitation. Indeed, the solution supersaturation increases with increasing the initial pH of the solution. This accelerates the nucleation and growth of $CaCO_3$. For example, at the initial solution pH 7, the supersaturation ratios with respect to calcite and vaterite are in the ranges $\sim$17–30 and $\sim$5–8, respectively. For the initial solution pH 9, $CaCO_3$ precipitation is instantaneous and the supersaturation ratios with respect to calcite and vaterite significantly increase, i.e., in the range $\sim$51–84 for calcite and in the range $\sim$14 –23 for vaterite. However, at constant supersaturation, it was shown that the growth rate of calcite decreases with increasing pH from 7.5 to 12 [41]. This is because the surface concentration of active growth sites decreases with increasing pH of the solution. Ramakrishna et al. [42] prepared $CaCO_3$ crystals by mixing Na_2, CO_3, and $CaCl_2$ solutions injected simultaneously into distilled water at different pH values. They showed that pure aragonite needles were formed at pH 10 and a mixture of calcite and aragonite was obtained when increasing the pH from 11 to 12. At high pH values, typically greater than 12, calcite was favored [43], and at pH lower than 8, vaterite was obtained [23]. Using a constant composition method, Tai and Chen [45] showed that vaterite was the predominant phase obtained, at 24°C, in the pH range 8.5−10, which is comparable to the precipitation pH range obtained when $CaCO_3$ was precipitated by the CO_2 repelling method (8.4−8.8) [16, 17]. For solution pH lower than 7–7.5, no precipitation of $CaCO_3$ was detected [17]. This result is of utmost importance in inhibiting $CaCO_3$ precipitation during scale formation in water and wastewater treatment processes, as will be discussed in the last paragraph of the present chapter.

5. Effect of foreign ions on $CaCO_3$ precipitation

The presence of mineral ions can significantly influence the crystal growth and microstructure of $CaCO_3$ [50–59]. Among mineral ions, sulphate and magnesium ions are widely studied [50, 53–59] since they are present at significant concentrations in natural waters. Compared to sulphate and magnesium ions, the impact of iron on the precipitation of calcium carbonate seems to be less studied and it

appears to be a lack of reliable data on its impact on $CaCO_3$ precipitation, especially at elevated temperature and different pH. **Figure 4** shows a tank highly containing iron-rich water. Iron ions can be present in the aqueous phase either from the corrosion of metallic parts in water desalination processes, such as tanks and pipes [60] or they may be present in groundwater at concentration levels depending on the mineral composition of the aquifer [61]. The water treatment processes are selected according to the water salt concentration. Indeed, membrane technological processes are used to desalinate brackish water containing salt concentrations below 10 g/L, however, reverse osmosis and thermal distillation are generally used to desalinate sea water with salt concentration above 30 g/L. Note that the typical iron concentration in the water used for the above mentioned processes is approximately 2.8 mg/L [62]. Groundwaters containing more than 0.2 mg/L of iron should be treated if used for drinking water [63]. Therefore, it is of great importance to understand how iron and calcium ions interact with each other during $CaCO_3$ precipitation. Throughout the followings, I put a special emphasis on the effects of magnesium, sulphate and iron ions on the precipitation kinetics, microstructure, and polymorphism of $CaCO_3$. Also, the mechanisms by which these ions affect the crystal growth of calcium carbonate were pointed out. Knowledge about the effects of these ions is very important in the elucidation of the growth polymorphs during water treatment.

5.1 Effect of magnesium and sulphate ions

It was shown that both sulphate and magnesium ions inhibit $CaCO_3$ crystallization [50, 55, 56], even though some discrepancies on the effect of sulphate ions were revealed. For example, at fixed temperature and ionic strength, Karoui et al. [50] showed that, the addition of sulphate ions to the $CaCO_3$ solution increased the induction time and decreased both the crystal growth rate and the amount of the precipitated $CaCO_3$. Comparable results were found by Vavouraki et al. [57]. However, Tlili et al. [64] showed that sulphate ions increase the growth rate of $CaCO_3$ precipitated electrochemically. Many works [51, 65, 66] have shown that sulphate ions inhibit vaterite transformation and enhance the calcite formation for low concentrations. At high concentrations, it was shown that sulphate ions

Figure 4.
A tank containing iron-rich water. Iron ions can be present in the aqueous phase either from the corrosion of metallic parts or they may be present in groundwater at concentration levels depending on the mineral composition of the aquifer.

(i) increased the nucleation time [50], (ii) decreased the precipitation rate of calcite formation [57] and (iii) promoted the formation of aragonite via a dissolution−precipitation process after long reaction times [55, 59].

The temperature and the ratio of magnesium to calcium control the precipitation kinetics, the type of polymorph and the morphology of the $CaCO_3$ precipitates [37, 64, 67]. For example, it was shown that when the Mg^{2+}/Ca^{2+} ratio passes from 0 to 4, with a Ca^{2+} concentration of 4×10^{-3} mol L^{-1}, the scaling time increases from 50 to 400 min, respectively [64]. Mejri et al. [37] studied the effect of magnesium ions on the $CaCO_3$ precipitation, by the CO_2 repelling method, at different temperatures between 30°C and 60°C and with different magnesium to calcium molar ratios (R) in the range 2–5. They showed that, at a fixed temperature, the increase of Mg^{2+} concentration significantly increased the induction time (t_n) and decreased both the initial crystal growth rate (V_i) and the amount precipitated (Rp). For example, at 40°C, t_n passed from 7 to 30 min, V_i passed from 0.57 to 0.49 M min^{-1} and Rp decreased from 81 to 56% when R passed from 0 to 5, respectively. The increase in temperature from 30–60°C weakens the impact of magnesium ions on the retardation of $CaCO_3$ precipitation. These results agree with previous works [38, 67–69], showing that the induction time significantly increased due to the presence of Mg^{2+}. At high concentrations of magnesium, amorphous $CaCO_3$ exhibited a prolonged stability, while it transformed instantly to calcite and vaterite in pure water [58]. In the presence of high amounts of Mg^{2+}, $CaCO_3$ exclusively precipitated as aragonite while calcite and vaterite formed when no Mg^{2+} ions are present [70]. At low temperature of 30°C, the addition of Mg^{2+} ions favored the crystallization in the bulk solution of secondary aragonite, resulted from the transformation of vaterite nuclei, while primary aragonite was favored, at high temperature of 60°C, with larger particles sizes than those obtained at 30°C [37].

5.2 Effect of iron ions

The results reported in literature on the effect of iron ions on $CaCO_3$ precipitation are often contradictory. For example, Kelland [71] found that iron ions concentrations below 25 ppm did not affect the $CaCO_3$ precipitation in high pressure dynamic tube blocking tests. Comparable results were found by Lorenzo et al. [72] who studied the effect of ferrous iron ions on the $CaCO_3$ growth by the constant composition method. However, Herzog et al. [73] found that, in magnetic water treatment devices, an excess of ferrous ions (5.6 ppm) strongly inhibits both calcite growth and the transformation of aragonite to calcite. The inhibiting effectiveness depends strongly on the solution supersaturation [16, 17, 74–76]. Indeed, at high supersaturations, the inhibition effectiveness of iron on $CaCO_3$ crystallization is small. In that case, the inhibition effectiveness can be improved by lowering the solution pH, increasing the iron concentration and/or by lowering the solution supersaturation [16, 17]. At relatively low supersaturations, the addition of iron ions retards the $CaCO_3$ precipitation. Past the onset of nucleation, iron ions enhance the growth rate of $CaCO_3$ and most of $CaCO_3$ amounts precipitate in the bulk solution instead of on the cell walls minimizing, therefore, the risks of scaling. Scaling is defined as the precipitation on the cell walls [16]. These results agree with those of Katz et al. [74] and Takasaki et al. [76] showing that lower supersaturations require less iron for the same extent of $CaCO_3$ growth inhibition.

It was shown [16] that for both temperatures 28°C and 50°C, the addition of iron retarded the nucleation of $CaCO_3$ and, most important, it decreased the $CaCO_3$ precipitation in the cell walls which can be easily collected, reducing therefore scale phenomena in water treatment devices. At a fixed temperature of 50°C, the increase in the iron concentration in the solution to 0.5 mg/FeL did not significantly affect

the $CaCO_3$ precipitation [17]. Comparable result was obtained by Macadam and Parsons [77] who showed that addition of 0.5 mg L^{-1} of iron did not affect the induction time of $CaCO_3$ precipitation by magnetic stirring at 40°C. For higher iron concentrations, the solution supersaturation decreased, and the inhibition effectiveness of iron ions became more pronounced [17]. At 50°C, the addition of iron ions in the solution promoted aragonite formation rather than vaterite. Indeed, with the increase in the iron ions concentration, the solution supersaturation decreased and the dissolution of vaterite became, most likely, faster which promotes aragonite formation. However, at 28°C, the addition of iron ions did not affect the nature of the precipitated phases vaterite and aragonite, and vaterite with rough surfaces was the predominant polymorph. This was explained that iron ions substituted partially Ca^{2+}, which inhibits vaterite dissolution and prevents the transformation of vaterite into aragonite [16, 17].

For a given iron concentration, increasing the initial pH causes the decrease in the induction time and the increase in the initial crystal growth rate. However, increasing iron ions concentration at a fixed pH in the range 7–9, results in the decrease in both the induction time and the crystal growth rate of $CaCO_3$ [17]. Additionally, the increase in iron ions concentration at a fixed pH reduced the amount of the precipitates obtained and, however, enhanced the precipitation of $CaCO_3$ in the bulk solution, reducing therefore the risks of scaling. Therefore, the $CaCO_3$ precipitation on cell walls, which causes the major phenomenon of scaling, could be lowered by enhancing the initial solution pH or by controlling the concentration of iron ions in the solution. However, the increase of the initial solution pH leads to high amounts of $CaCO_3$ precipitates and even when formed in the bulk solution, they can agglomerate and block up different parts of the water treatment devices such as pipes and conducts, resulting in the blockage of fluid cooling. This increases processing costs, decreases equipment life, and decreases the product water recovery.

At 28°C and initial pH 8, calcite and vaterite were obtained. The increase in iron concentration in the solution resulted in an increased formation of calcite. At initial pH 9 and iron concentration of 4 mg/FeL, calcite was the only phase detected. At 28°C, the increase of the initial solution pH resulted in the disappearance of aragonite and the precipitation of vaterite and calcite. Iron ions addition up to 4 mg/FeL accelerated the transformation of vaterite into calcite and only calcite with stepped surfaces (**Figure 5**) was obtained at initial pH 9 [17]. The stepped surfaces were explained by iron ions adsorption or to difficulties in incorporating building units into the surfaces of calcite crystals [78].

5.3 Effect of chloride ions

For high concentrations, chloride might affect the stability of calcium in the solution, and thus the precipitation of $CaCO_3$. However, at relatively low temperatures between 15°C and 85°C, the equilibrium association constants of calcium ions with chloride ions in aqueous solution reported in literature are small. In fact, log$K$ varies between -0.28 and -0.04 [79–83] which indicates, therefore, the instability of the ion pairs. Korchef and Touabi [17] showed that, at 28 and 50°C and for low concentrations of chloride below 0.18 mM, calcium chloride ion pairs either do not form or have stability fields too small to remarkably decrease the free calcium ion concentration in the solution and to reduce, therefore, the $CaCO_3$ growth rate. Calcium chloride ion pairs form at higher temperatures, i.e., for temperatures in the range 100-360°C, the stability field for $CaCl^+$ decreases with enhancing temperature, whereas that for $CaCl_2^0$ increases significantly [84]. It should be noted that higher order calcium chloride ion pairs do not form or have small stability fields.
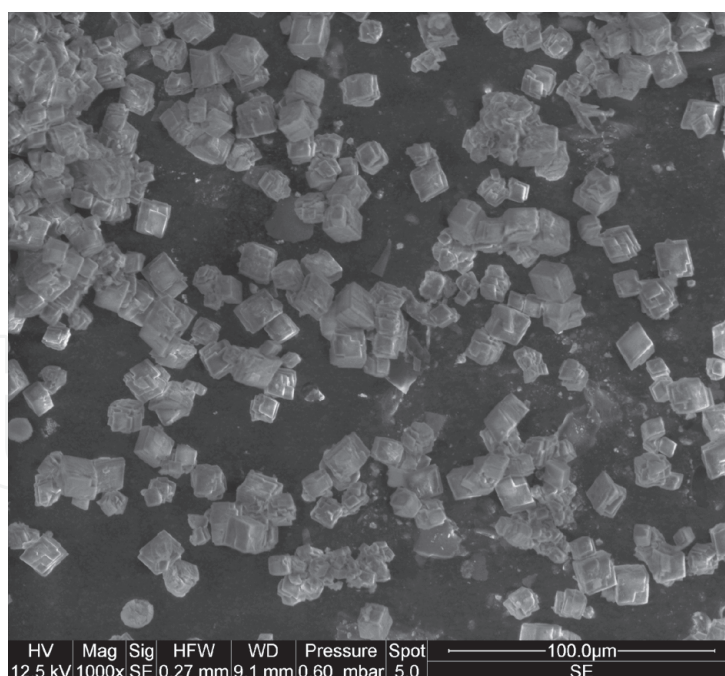
Figure 5.
Calcite with stepped surfaces obtained at 28°C, initial solution pH 9, and iron ions concentration of 4 mg/FeL.

In addition, chloride ions can be added as sodium chloride NaCl. Tai and Chen [45] studied the effect of ionic strength and additives concentration on the polymorphism of $CaCO_3$ formed in a constant composition environment. They adjusted the ionic force by NaCl addition which is, they found, inactive in the polymorphic form. Moreover, Takita et al. [85] showed that low concentrations of NaCl in the range 0.1–0.5 M did not remarkably affect the solubility of $CaCO_3$. However, when an excess of NaCl (2.5 M) was added, the solubility of $CaCO_3$ increased which promoted the vaterite to calcite transformation. The resulting high concentration of $CaCO_3$ favored crystal growth rather than nucleation.

5.4 Effect of additives and dissolved organic matter

Ukrainczyk et al. [86] investigated the effect of salicylic acid derivatives on calcite precipitation kinetics and morphology. Their results showed that the adsorption of additive molecules lowered the $CaCO_3$ growth rate by blocking the propagation of growth sites. This causes the formation of steps and jagged and discontinuous surfaces. Comparable results were obtained for magnesium-containing solutions, where calcite crystal edges were rough and growth steps were apparent [55]. Comparable effects were also found when iron was added [16, 17]. The presence of additives, such as monoethylene glycol (MEG), prevents the vaterite to calcite transformation and stabilizes the formation of the relatively unstable vaterite polymorph. For example, Natsi et al. [87] showed that, in the presence of low concentrations of MEG of (10−20% v/v), vaterite was stabilized. At stable supersaturated solutions, seeded with quartz and calcite crystals, the growth of $CaCO_3$ was significantly reduced with the increase of MEG concentrations. At 60% of MEG, the vaterite/aragonite- to-calcite transformation was prevented, whatever the synthesis temperature [88].

On the other hand, it was shown that dissolved organic matter (DOM) inhibits $CaCO_3$ crystal growth [89]. The inhibition effect was related to the formation of calcium complexes and the occupation of the $CaCO_3$ growth sites which resulted in $CaCO_3$ rough surfaces. Dzacula et al. [90] studied in vitro precipitation of aragonite

in artificial seawater at a high supersaturation of 11, and at a low supersaturation of 5.8. In either chemical systems, different concentrations of soluble organic matter (SOM), extracted from the symbiotic coral B. europea (SOM-Beu) and the a-symbiotic one L. pruvoti (SOMLpr) were added in order to investigate their effect on crystal growth or nucleation processes. They showed that, at high supersaturation, the SOMs increased the induction time but did not change the growth rate, and they were incorporated within nanoparticles aggregates. At low supersaturation, the SOMs affected the overgrowing crystalline unit aggregation and did not substantially affect the growth rate.

6. Possible mechanisms

According to the Ostwald [91] law, the least stable phase, that has the highest solubility, precipitates first and subsequently transforms to the more stable one. This transformation can be either a solid-state transition that invokes internal rearrangements of atoms, ions or molecules [92, 93] or a solution mediated transformation that invokes the dissolution of the metastable phase in the solution and simultaneous precipitation of the stable phase [94, 95]. It was shown that the amorphous calcium carbonate is a precursor in spontaneous precipitation of $CaCO_3$ at relatively high supersaturations. The amorphous phase, which consists of spherical particles with the diameter in the range 50–400 nm, dissolves rapidly in an undersaturated solution and it undergoes a rapid transformation to one of the more stable anhydrous forms (calcite, vaterite and aragonite) [4]. Therefore, the unstable amorphous calcium carbonate is firstly formed [36]. Then, it transforms into crystalline phases which are vaterite, calcite and aragonite. The vaterite can be transformed gradually into calcite or aragonite following two steps that are (i) the vaterite dissolution and (ii) the calcite or aragonite growth [71]. The second step controlled the overall rate of vaterite transformation to the most stable phase calcite or aragonite [96]. The two hydrated crystalline forms of calcium carbonate, calcium carbonate hexahydrate $CaCO_3 \cdot 6H_2O$ and calcium carbonate monohydrate $CaCO_3 \cdot H_2O$, are more stable than the amorphous $CaCO_3$. Calcium carbonate monohydrate crystallized in well-defined spherical crystals with diameters in the range 15–30 mm and calcium carbonate hexahydrate crystallizes in well-defined rhombohedral crystals in the size range between 10 and 40 mm. Generally, hydrated forms precipitate from supersaturated solutions before the more stable anhydrous forms calcite, vaterite and aragonite [4].

As shown above, both sulphate and magnesium ions inhibit $CaCO_3$ crystallization [50, 55, 56]. The inhibition effect of magnesium ions was explained by (i) the increase in calcite solubility induced by magnesium ions insertion into the calcite crystals by substituting calcium ions [97]. This substitution depends on the Mg^{2+}, Ca^{2+} and SO_4^{2-} ions concentrations [50], (ii) accumulated strain provoked by smaller magnesium ions incorporation [50, 56] and (iii) adsorption of magnesium ions on calcite surfaces [56]. Indeed, based on the calculation of defect-forming energies in the crystalline lattice of aragonite, Mandakis et al. [98] showed that Mg^{2+} ions can substitute Ca^{2+} ions. This substitution may take place in the volume of the orthorhombic lattice of aragonite or on the crystal surfaces. Assessing the mechanism by which Mg^{2+} ions act to inhibit the crystalline growth of $CaCO_3$ requires an understanding of the changes that must occur when an ion is transferred from the solution to its location in the crystalline lattice. In the solution, Mg^{2+} ions are surrounded by six molecules of H_2O [99]. The incorporation of Mg^{2+} ions implies therefore the replacement of the H_2O molecules by six carbonate groups of the $CaCO_3$ lattice. This is done by partial dehydration (replacement of three H_2O molecules by oxygen from

the calcite lattice) and then diffusion to a growth site and total dehydration (replacement of the three remaining H_2O molecules) [99]. According to Folk [100], the adsorption and incorporation of Mg^{2+} ions into the calcite lattice leads to the distortion of the crystalline lattice because of the lower ion radius of Mg^{2+} than that of Ca^{2+} (**Figure 6**). Thus distorted, the crystalline structure of the calcite can no longer accept the following Ca^{2+}, which comes to seek its position in the $CaCO_3$ lattice. Therefore, the crystalline growth of calcite is inhibited. This results in a solubility of calcite containing Mg^{2+} ions greater than that of pure calcite (without Mg^{2+}) [101].

Sulphate ions can be incorporated into the $CaCO_3$ lattice structure. Kitano et al. [97] demonstrated that this incorporation is easier in calcite than in aragonite and that with the increase in NaCl concentration in the solution, the sulphate ions content in calcite decreases significantly while in aragonite it remains constant. A simple model that describes the incorporation of sulphate into the calcite lattice was proposed by Kontrec et al. [102]. In this model, a carbonate group can be replaced by sulphate. Three oxygen atoms of the tetrahedral sulphate structure, which occupies an area of 256.4 $Å^2$, are accommodated in place of the planar carbonate group occupying a smaller surface area of 212.1 $Å^2$. Sulfur and the fourth oxygen of the sulphate group are outside the carbonate plane. As a result, this substitution causes the crystalline lattice of calcite to be distorted. The distortion on the c-axis is more important than on the other two axes (a and b). A comparable model was proposed for the incorporation of sulphate ions into the orthorhombic structure of aragonite [50, 51]. In addition, sulphate ions can be adsorbed on the $CaCO_3$ surfaces [50]. This adsorption was explained by a mechanism involving a change in the surface charge of $CaCO_3$ and a contribution of the Ca^2 ions to the release of carbonate ions from the surface of $CaCO_3$. Indeed, Strand et al. [103] showed that the negatively charged carbonate ions are released from the surface of $CaCO_3$ (desorption) which leads to a positively charged surface. It should be noted that the causes of this desorption have not been mentioned but it was shown that, using a measure of zeta potential, sulphate and calcium ions generate the properties of the $CaCO_3$/water interface. The sulphate ions are adsorbed on this surface and the released carbonate ions react with the Ca^{2+} ions to form $CaCO_3$ on this same surface (**Figure 7**). This adsorption increases with temperature and/or Ca^{2+} ion concentration [103].

The inhibitory effectiveness of iron ions on $CaCO_3$ nucleation, and growth was generally attributed to that (i) iron ions are blocking the growth sites of $CaCO_3$ by incorporating the growing layers, which leads to a strained lattice where calcium ions no longer fit [72] (ii) the formation of colloidal iron oxides, i.e., Fe_2O_3 [104] (iii) iron precipitates mainly in the form of siderite, which acts as heterogeneous sites for $CaCO_3$ precipitation and improves the scale inhibition effectiveness.

The formation of iron oxides and their interactions with $CaCO_3$ remain controversial. For example, experiments were conducted by Herzog et al. [73] on various forms of ferric hydroxide to test if a form is effective for the heterogeneous nucleation of $CaCO_3$. They found that the tested forms of iron hydroxides or
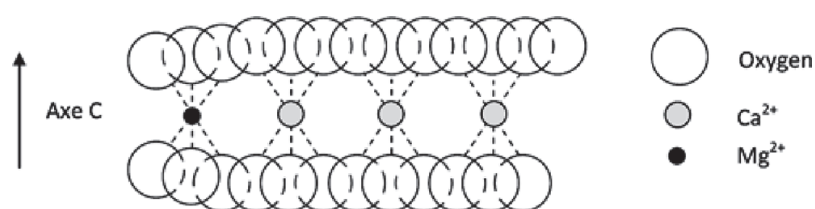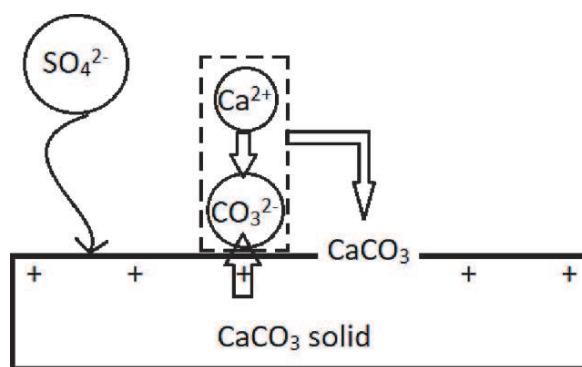

Figure 6.
Calcite lattice distortion due to the incorporation of Mg^{2+}.

Figure 7.
Schematic illustration of the adsorption of sulphate ions on the surfaces of CaCO₃.

hydrated iron oxides did not have any effect on $CaCO_3$ nucleation and growth. This disagrees with the results of Mejri et al. [105]. In fact, they studied the $CaCO_3$ precipitation in 2 mM $Ca(HCO_3)_2$ solution in the presence of iron ions concentrations between 5 and 20 mg L^{-1}. They showed that iron ions addition promotes $CaCO_3$ precipitation. This was attributed to the formation of iron hydroxide before the onset of $CaCO_3$ precipitation which plays a role of seed and initiates the $CaCO_3$ nucleation. Coetzee et al. [104] showed that the addition of iron had a small effect on the crystal morphology but reduced the induction times. The enhanced nucleation rates were explained by the formation of hematite Fe_2O_3 colloids that act as seed crystals and increase the heterogeneous nucleation process. What is more, it was shown that the presence of Fe^{2+} ions in contact with calcite surfaces accelerates calcite dissolution sites during its oxidation and co-precipitation onto calcite surfaces as ferric iron hydroxide, which was rapidly transformed into FeOOH nanoparticles [61]. Thus, the water being treated can be softened by iron precipitation and the final product can be reused as mineral filler powders or as a pigment for industrial applications.

The formation of siderite $FeCO_3$ on the $CaCO_3$ surfaces blocks growth sites and/or forms a protection layer. This layer retards the $CaCO_3$ precipitation and decreased the corrosion rate of mild steel in simulated saline aquifer environments [106]. The formation of siderite, before the onset $CaCO_3$ precipitation, was experimentally observed by scanning electron microscopy [16]. $FeCO_3$ was formed at relatively low supersaurations and serves as a seed for heteronucleation of vaterite. At high supersaturations, however, $FeCO_3$ either does not form or has stability fields too small to remarkably affect the $CaCO_3$ precipitation. In fact, it was shown that $CaCO_3$ crystallizes in higher amounts than $FeCO_3$ in a solution supersaturated with respect to both $FeCO_3$ and $CaCO_3$ [107], and $FeCO_3$ precipitation is not probable, at high supersaturations, because calcium ions increase the solubility of $FeCO_3$ decreasing, therefore, its precipitation rate [107, 108]. It was shown that, when the carbonate system presents relatively high concentrations, iron solubility is controlled by $FeCO_3$ rather than by $Fe(OH)_2$ in CO_2 saturated solutions [109]. This was confirmed by Korchef's work [16]. Indeed, according to Korchef's mechanism [16], $FeCO_3$ forms first from amorphous iron hydroxide, i.e., consistent with the so-called nonclassical nucleation theory [110] and then serves as a template for heteronucleation of $CaCO_3$. When the concentration of the iron ions increases, the amount of $FeCO_3$ formed increases, which increases the number of heterogeneous sites and enhances the inhibition effectiveness of scale. Then, $FeCO_3$ could be incorporated in a solid solution $Fe_xCa_{1-x}CO_3$ ($0 \leq x \leq 1$) by a solid–solid transition (**Figure 8**). Indeed, the solids $CaCO_3$ and $FeCO_3$ are isostructural, and their constituent cations (Ca^{2+} and Fe^{2+}) can coexist, as a mixed metal carbonate, in the

substitutional solid solution $Fe_xCa_{1-x}CO_3$ [108]. The $FeCO_3$ dissolution was recently reported by Rizzo et al. [111] who studied the effect of $CaCO_3$ precipitation on the corrosion of carbon steel, covered by a protective $FeCO_3$ layer. The authors showed that $CaCO_3$ precipitation lead to an undersaturated solution with respect to $FeCO_3$ followed by dissolution of the protective $FeCO_3$ layer. The partial substitution of Ca^{2+} by Fe^{2+} suppresses the transformation of vaterite into aragonite which results in the decrease of the aragonite amount with increasing iron ions
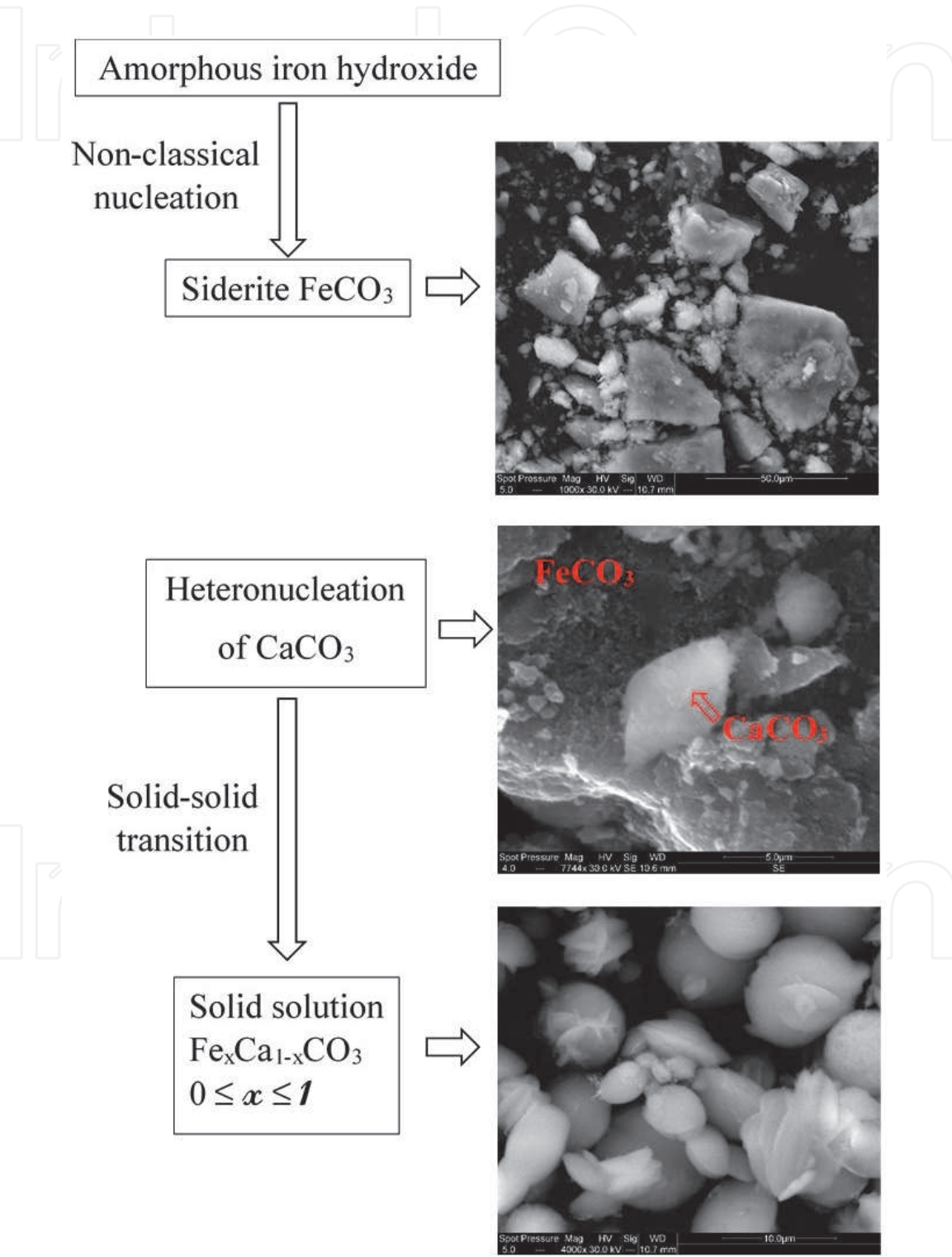

Figure 8.
Korchef's mechanism [16]: In iron-rich water, siderite ($FeCO_3$) form first from amorphous iron hydroxide, consistent with the so-called nonclassical nucleation theory and then serves as a template for heteronucleation of $CaCO_3$. Next, siderite is incorporated in $Fe_xCa_{1-x}CO_3$ ($0 \leq x \leq 1$) solid solution by a solid–solid transition.

concentration. Comparable results were found for Fe(II), [75] Fe(III), [74, 76] and Zn(II) [112]. In fact, Zn(II) precipitated mainly as $ZnCO_3$ which, like siderite, acts as heterogeneous sites in the bulk of solution and decreased the number of crystals on the surface. As a result, scale is reduced [112].

It is worth noticing that, since $FeCO_3$ precipitates at lower pH values than $CaCO_3$ [16], maintaining the solution pH at relatively low values (<7) allowed obtaining only $FeCO_3$. $FeCO_3$ can form protective film on different steel parts of industrial processes which, reduces or completely prevents their corrosion. This reduces remarkably the treatment costs and increases the equipment life.

7. Scale inhibition

Al-Hamza et al. [113] studied the inhibition effect of poly(acrylic acid) (PAA) with different end groups and molar masses on the formation of $CaCO_3$ scale at low and high temperatures. They showed that the inhibition of $CaCO_3$ precipitation was affected by the hydrophobicity of the end groups of PAA. The best inhibition was found for PAA with hydrophobic end groups of moderate size (6–10 carbons). Also, the scale inhibitors stabilize the less thermodynamically stable polymorph (vaterite) to a degree proportional to their ability to inhibit precipitation. At room temperature, the lowest molar mass of PAA with hydrophilic end group showed good efficiency in the inhibition of $CaCO_3$ precipitation making it suitable to be used as a scale inhibitor in reverse osmosis desalination. However, the lowest molar mass PAA with end groups of moderate hydrophobicity are more suitable as scale inhibitors in MSF desalination. The effectiveness of the inhibitors declined with increasing temperature. Comparable results were found by Li et al. [114] who studied the scale inhibition effect of six varieties of commercial scale inhibitors in highly saline conditions at high temperature. Indeed, they showed that the inhibition efficiency was influenced by scale inhibitor dosage, temperature, heating time and pH. The best scale inhibitor (SQ-1211) could effectively retard scaling at high temperature and when the concentration of Ca^{2+} was 1600 mg L^{-1}, the scale inhibition rate reached 90.7% at 80°C and pH 8. The crystal structure of $CaCO_3$ changed from calcite to aragonite. Xu et al. [115] studied the inhibition of $CaCO_3$ scaling on stainless steel surfaces using sodium carboxymethyl cellulose (SCMC). They showed that SCMC exhibited a promising performance of scaling inhibition, and the inhibition efficiency increased with increasing SCMC concentration starting from 50 to 200 mg L^{-1}. For example, the inhibition efficiency reached 93.2% for SCMC concentration of 200 mg L^{-1}. The inhibition effect was explained by the formation of a protective film on the stainless-steel surfaces by adsorption of the constituent of SCMC in the presence of SCMC, preventing the deposition of $CaCO_3$. Zuho et al. [116] investigated the feasibility of electrochemical methods to study the scale inhibition performance of 1-hydroxyethylidene-1,1-diphosphonic acid (HEDP) and 2-phosphonobutane-1,2,4-tricarboxylic acid (PBTCA), polyacrylic acid (PAA) on titanium surfaces. They showed that, for electrochemically deposited $CaCO_3$ scale, PBTCA, HEDP and PAA have great inhibitory effects and the order of the scale inhibition efficiency of the three inhibitors is PBTCA > HEDP > PAA. The deposition of $CaCO_3$ on the surface of TA1 metal mainly results in dendritic aragonite crystals and when scale inhibitors were added, the aragonite crystal polymorph was gradually modified to vaterite. Yu et al. [117] designed and prepared phosphorus-free and biodegradable scale inhibitors. In fact, two series of starch-*graft*-poly(acrylic acid) (St-*g*-PAA) samples with different grafting ratios and grafted-chain distributions, that are, the number and length of grafted PAA chains

on the starch backbone were elaborated. They showed that St-*g*-PAA with relatively low grafting ratio (typically ≤97%) inhibited scale formation more effectively than samples with similar grafted-chain distributions. However, under the similar grafting ratios, samples with higher number of branched chains with shorter grafted chains showed better scale efficiency.

More interesting, Korchef and Touabi [17] showed that high amounts of precipitates were obtained with increasing the initial solution pH, and even when formed in the bulk solution, these precipitates can agglomerate and block up pipes pumps and conducts of water in water treatment devices leading to the complete blockage of fluid cooling. For solution pH lower than 7–7.5, no precipitation of $CaCO_3$ was detected [17]. For that reason, the solution pH should be maintained at low values (pH below 7). This can be easily achieved by avoiding CO_2 repelling from the solution. This allows reducing or completely preventing scale in different water treatment processes and favorably affects the water treatment costs and increases the equipment life. In practice, this is achievable by avoiding the contact between water and the atmospheric air. For example, in the desalination units using the solar multiple condensation evaporation cycle (SMCEC) principle, the supersaturation of the feed water increases remarkably with the number of the condensation–evaporation cycles [15] and accordingly, it is expected that iron ions do not inhibit the formation of $CaCO_3$ as scale in the SMCEC desalination units. In that case, it is mandatory to regulate the pH of feed water below 7 to prevent scale formation.

8. Conclusion

Water desalination processes such as reverse osmosis, electrodialysis and distillation are confronted with scale formation which causes enormous energy losses and shortens the equipment life. In most cases, scales are made of $CaCO_3$ which possesses six polymorphs. Environmental conditions play effective roles in the nucleation and growth kinetics of $CaCO_3$ as well as the morphology and polymorphism of the obtained precipitates. In the present chapter, an overview on the effect of operating conditions such as supersaturation, temperature, and pH, on the crystal growth and microstructure of $CaCO_3$ is given. Additionally, I put special emphasis on the effect of foreign ions, especially magnesium, sulphate, chloride, and iron ions. Also, the mechanisms by which these ions affect the crystal growth of $CaCO_3$ were pointed out. The experimental parameters should operate together and control the growth rate and polymorphism of $CaCO_3$. Throughout the present chapter, it was reported that:

- the unstable amorphous $CaCO_3$ is firstly formed. Then, it transformed into crystalline phases which are namely vaterite, aragonite and calcite. The vaterite can be transformed gradually into calcite or aragonite following two steps which are the dissolution of vaterite and the growth of calcite or aragonite. The dissolution of vaterite is affected by the presence of foreign ions, i.e., magnesium, sulphate, and irons ions. The two hydrated crystalline forms of calcium carbonate, calcium carbonate hexahydrate $CaCO_3 \cdot 6H_2O$ and calcium carbonate monohydrate $CaCO_3 \cdot H_2O$, are more stable than the amorphous $CaCO_3$.

- the crystal growth rate of $CaCO_3$ increases with increasing the solution supersaturation.

- the increase of temperature results to the decrease of the induction time and to the increase of the growth rate of $CaCO_3$ and, also the amount precipitated. At room temperature, calcite is the most predominant phase. At temperatures higher than 50°C, $CaCO_3$ scale precipitates as needles-like aragonite crystals.

- the increase of the initial solution pH accelerates the $CaCO_3$ precipitation. For solution pH lower than 7–7.5, no precipitation of $CaCO_3$ was detected. At pH lower than 8, vaterite was obtained. Pure aragonite needles were formed at pH 10 and a mixture of calcite and aragonite was obtained when increasing the pH from 11 to 12. At high pH values, typically greater than 12, calcite was favored.

- both sulphate and magnesium ions inhibit $CaCO_3$ crystallization, even though some discrepancies on the effect of sulphate ions were revealed.

- iron ions inhibit the $CaCO_3$ growth. The inhibiting effectiveness depends strongly on the solution supersaturation. At relatively low supersaturations, the addition of iron ions retards the $CaCO_3$ precipitation crystals. Past the onset of nucleation, iron ions increased the $CaCO_3$ growth rate and most of $CaCO_3$ amounts precipitated in the bulk solution rather than on the cell walls. This results in the decrease of scaling defined as the precipitation on the cell walls. At high supersaturations, the inhibition effectiveness of iron is small. In that case, the inhibition effectiveness can be enhanced by controlling the operating parameters, i.e., lowering the solution pH, increasing the iron concentration, and/or lowering the solution supersaturation.

- the control of the operating parameters and the water composition allows completely inhibiting or, at least, reducing scale formation in various industrial devices such as desalination units and heat exchangers.

- in practice, the solution pH should be maintained at low values (below 7) by avoiding CO_2 removal from the solution which allows reducing or completely preventing scale. This is realizable by preventing the contact between water and the atmospheric air. The economic impact is of greatest importance since this reduces considerably the treatment costs, enhances the equipment life, and allows increased product water recovery.

Acknowledgements

Conflict of interest

The author declares no conflict of interest.

Author details

Atef Korchef[1,2]

1 Joint Programs, College of Science, King Khalid University (KKU), Abha, Saudi Arabia

2 LVMU, Centre National de Recherches en Sciences des Matériaux, Technopole de Borj-Cédria, Tunisia

*Address all correspondence to: akorchef@kku.edu.sa

IntechOpen

References

[1] Huang Y, Ji Y, Kang Z, Li F, Ge S, Yang DP, et al. Integrating Eggshell-derived $CaCO_3$/MgO Nanocomposites and Chitosan into a Biomimetic Scaffold for Bone Regeneration. Chem. Eng. J. 2020;**395**:125098. DOI: 10.1016/j.cej.2020.125098

[2] Abbaszadeh M, Nasiri M, Riazi M. Experimental investigation of the impact of rock dissolution on carbonate rock properties in the presence of carbonated water. Environ. Earth Sci. 2016;**75**:791. DOI: 10.1007/s12665-016-5624-3

[3] Kalita JM, Chithambo ML. Thermoluminescence and infrared light stimulated luminescence of limestone ($CaCO_3$) and its dosimetric features. Appl. Radiat. Isot. 2019;**154**: 108888. DOI: 10.1016/j.apradiso.2019.108888

[4] Brečević L, Kralj D. On Calcium Carbonates: from Fundamental Research to Application. Croat. Chem. Acta. 2007;**80**:467-484

[5] Charde SJ, Sonawane SS, Sonawane SH, Navin S. Influence of functionalized calcium carbonate nanofillers on the properties of melt-extruded polycarbonate composites. Chem. Eng. Commun. 2018;**205**: 492-505. DOI: 10.1080/00986445.2017.1404459

[6] Hao BL, Lang Y, Bian DQ, Wang CA. Preparation of near net size porous alumina-calcium aluminate ceramics by gelcasting-pore-forming agent processs. J. Am. Ceram. Soc. 2020;**103**:4602-4610. DOI: 10.1111/jace.17075

[7] Souyris F, Pellequer C, Payrot C, Servera C. Coral, a new biomedical material. Experimental and first clinical investigations on Madreporaria. J. Maxillofac. Surg. 1985;**13**:64-69. DOI: 10.1016/s0301-0503(85)80018-7

[8] Fujioka-Kobayashi M, Tsuru K, Nagai H, Fujisawa K, Kudoh T, Ohe G, et al. Fabrication and evaluation of carbonate apatite-coated calcium carbonate bone substitutes for bone tissue engineering. J. Tissue Eng. Regen. M. 2018;**12**:2077-2087. DOI: 10.1002/term.2742

[9] Woldetsadik AD, Sharma SK, Khapli S, Jagannathan R, Magzoub M. Hierarchically Porous Calcium Carbonate Scaffolds for Bone Tissue Engineering. ACS Biomater. Sci. Eng. 2017;**3**:2457 2469. DOI: 10.1021/acsbiomaterials.7b00301

[10] Elsayed H, Picicco M, Ferroni L, Gardin C, Zavan B, Bernardo E. Novel bioceramics from digital light processing of calcite/acrylate blends and low temperature pyrolysis. Ceram. Int. 2020;**46**:17140-17145. DOI: 10.1016/j.ceramint.2020.03.277

[11] Braye F, Irigaray JL, Jallot E, Oudadesse H, Weber G, Deschamps N, et al. Resorption kinetics of osseous substitute: natural coral and synthetic hydroxyapatite. Biomaterials. 1996;**17**: 1345-1350. DOI: 10.1016/s0142-9612(96)80013-5

[12] Brecevic L. Nielsen AE. Solubility of amorphous calcium carbonate. J. Cryst. Growth. 1989;**98**:504-510. DOI: 101016/0022-0248(89)90168-1

[13] Helalizadeh A, Müller-Steinhagen H, Jamialahmadi M. Mixed salt crystallisation fouling. Chem. Eng. Process. 2000;**39**:29-43. DOI: 101016/S0255-2701(99)00073-2

[14] Mwaba MG, Golriz MR, Gu J. A semi-emperical correlation for crystallisation fouling on heat exchange surfaces. Appl. Therm. Eng. 2006;**26**: 440-450. DOI: 101016/japplthermaleng200505021

[15] Tlili MM, Korchef A, Ben Amor M. Effect of scalant and antiscalant concentrations on fouling in a solar desalination unit. Eng Process. 2007;**46**: 1243-1250. DOI: 101016/jcep200610006

[16] Korchef A. Effect of Iron Ions on the Crystal Growth Kinetics and Microstructure of Calcium Carbonate. Cryst. Growth Des. 2019;**19**:6893-6902. DOI: 101021/acscgd9b00503

[17] Korchef A, Touaibi M. Effect of pH and temperature on calcium carbonate precipitation by CO_2 removal from iron-rich water. Water Environ. J. 2020;**34**: 331-341. DOI: 101111/wej12467

[18] Pytkowicz RM. Rates of inorganic calcium carbonate precipitation. J. Geol. 1965;**73**:196-199. DOI: 10.1086/627056

[19] Cosmo RP, Pereira FAR, Ribeiro DC, Barros WQ, Martins AL. Estimating CO_2 degassing effect on $CaCO_3$ precipitation under oil well conditions. J. Petrol. Sci. Eng. 2019;**181**: 106207. DOI: 10.1016/j. petrol.2019.106207

[20] Hasan BO. Galvanic corrosion of aluminum–steel under two-phase flow dispersion conditions of CO_2 gas in $CaCO_3$ solution. J. Petrol. Sci. Eng. 2015;**133**: 76-84. DOI: 10.1016/j.petrol.2015.05.007

[21] Rizzo R, Gupta S, Rogowska M, Ambat R. Corrosion of carbon steel under CO2 conditions: Effect of CaCO3 precipitation on the stability of the $FeCO_3$ protective layer. Corros. Sci. 2020;**162**:108214. DOI: 10.1016/j. corsci.2019.108214

[22] Gopinath CS, Hegde SG, Ramaswamy AV, Mahapatra S. Photoemission studies of polymorphic $CaCO_3$ materials. Mater. Res. Bull. 2002; **37**:1323-1332. DOI: 10.1016/S0025-5408 (02)00763-8

[23] Han YS, Hadiko G, Fuji M, Takahashi M. Factors affecting the phase and morphology of $CaCO_3$ prepared by a bubbling method. J. Eur. Ceramic Soc. 2006;**26**:843-847. DOI: 10.1016/j.jeurceramsoc.2005.07.050

[24] Blue CR, Giuffre A, Mergelsberg S, Han N, DeYoreo JJ, Dove PM. Chemical and physical controls on the transformation of amorphous calcium carbonate into crystalline $CaCO_3$ polymorphs. Geochim. Cosmochim. Acta. 2017;**196**:179-196. DOI: 10.1016/j. gca.2016.09.004

[25] Miyazaki T, Arii T, Shirosaki Y. Control of crystalline phase and morphology of calcium carbonate by electrolysis: Effects of current and temperature. Ceram. Int. 2019;**45**: 14039-14044. DOI: 10.1016/j. ceramint.2019.04.103

[26] Jimoh OA, Ariffin KS, Hussin HB, Temitope AE. Synthesis of precipitated calcium carbonate: A review. Carbonate Evaporite. 2018;**33**:331-346. DOI: 10.1007/s13146-017-0341-x

[27] Plummer LN, Busenberg E. The solubility of calcite, aragonite and vaterite in solutions between 0 and 90°C and an evaluation of the aqueous model for the system $CaCO_3$-CO_2-H_2O. Geochim. Cosmochim. Acta. 1982;**46**: 1011-1040. DOI: 10.1016/0016-7037 (82)90056-4

[28] Konopacka-Łyskawa D. Synthesis methods and favorable conditions for spherical vaterite precipitation: A review. Crystals. 2019;**9**:223. DOI: 10.3390/cryst9040223

[29] Akhtar K, Yousafzai S. Morphology control synthesis of nano rods and nano ovals $CaCO_3$ particle systems. J. Disper. Sci. Technol. 2020;**41**:1-15. DOI: 10.1080/01932691.2019.1626248

[30] Rom I, Klas S. Kinetics of $CaCO_3$ precipitation in seeded aeration softening of brackish water desalination concentrate. Chemosphere. 2020;**260**:

127527. DOI: 10.1016/j. chemosphere.2020.127527

[31] Haaring R, Kumar N, Bosma D, Poltorak L, Sudhölter EJR. Electrochemically Assisted deposition of calcite for application in surfactant adsorption studies. Energ. Fuels. 2019; **33**:805-813. DOI: 10.1021/acs. energyfuels.8b03572

[32] Alimi F, Tlili MM, Gabrielli C, Maurin G, Ben Amor M. Effect of a magnetic water treatment on homogeneous and heterogeneous precipitation of calcium carbonate. Water Res. 2006;**40**:1941-1950. DOI: 10.1016/j.watres.2006.03.013

[33] Roques H. Chemical Water Treatment: Principles and Practice. New York: VCH; 1996

[34] Hamer WJ. Theoretical mean activity coefficients of strong electrolytes in aqueous solutions from 0 to 100 °C. US. Natl. Bur. Stand., Ref. Data Ser. 1968;**24**:271

[35] Truesdell AH, Jone BFA. Computer program for calculating chemical equilibria of natural waters. U.S. Geol. Survey J. Res. 1974;**2**:233-–274

[36] Elfil H, Roques H. Prediction of the limit of the metastable zone in the $CaCO_3$-CO_2-H_2O system. AIChE J. 2004;**50**:1908-1916. DOI: 10.1002/ aic.10160

[37] Mejri W, Korchef A, Tlili MM, Ben Amor M. Effects of temperature on precipitation kinetics and microstructure of calcium carbonate in the presence of magnesium and sulphate ions. Desalin. Water Treat. 2014;**52**: 4863-4870. DOI: 10.1080/ 19443994.2013.808813

[38] Söhnel O, MullinJ W. Precipitation of calcium carbonate. J. Cryst. Growth. 1982;**60**:239-250. DOI: 10.1016/ 0022-0248(82)90095-1

[39] Chen J, Xiang L. Controllable synthesis of calcium carbonate polymorphs at different temperatures. Powder Technol. 2009;**189**:64-69. DOI: 10.1016/j.powtec.2008.06.004

[40] Weiss JCA, Cancel KT, Moser RD, Allison PG, Gore ER, Chandler MQ, et al. Influence of temperature on calcium carbonate polymorph formed from ammonium carbonate and calcium acetate. J. Nanotech Smart Mater. 2014; **1**:1-6

[41] Ruiz-Agudo E, Putnis CV, Rodriguez-Navarro C, Putnis A. Effect of pH on calcite growth at constant aCa^{2+}/ aCO_3^{2-} ratio and supersaturation. Geochim. Cosmochim. Acta. 2011;**75**: 284-296. DOI: 10.1016/j.gca.2010.09.034

[42] Ramakrishna C, Thenepalli T, Huh JH, Ahn JW. Precipitated calcium carbonate synthesis by simultaneous injection to produce nanowhisker aragonite. J. Korean Ceram. Soc. 2016; **53**:222-226. DOI: 10.4191/ kcers.2016.53.2.222

[43] Chang R, Kim S, Lee S, Choi S, Kim M, Park Y. Calcium carbonate precipitation for CO_2 storage and utilization: A review of the carbonate crystallization and polymorphism. Front Energy Res. 2017;**5**:1-–12. DOI: 10.3389/ fenrg.2017.00017

[44] Kralj D, Brečević L, Nielsen AE. Vaterite growth and dissolution in aqueous solution. I. Kinetics of crystal growth. J. Cryst. Growth. 1990;**104**: 793-800. DOI: 10.1016/0022-0248(90) 90104-S

[45] Tai CY, Chen FB. Polymorphism of $CaCO_3$ precipitated in a constant-composition environment. AIChE J. 1998;**44**:1790-1798. DOI: 10.1002/ aic.690440810

[46] Chen J, Xiang L. Controllable synthesis of calcium carbonate polymorphs at different temperatures.

Powder Technol. 2009;**189**:64-69. DOI: 10.1016/j.powtec.2008.06.004

[47] Gabrielli C, Maurin G, Poindessous G, Rosset R. Nucleation and growth of calcium carbonate by an electrochemical scaling process. J. Cryst. Growth. 1999;**200**: 236-250. DOI: 10.1016/S0022-0248(98) 01261-5

[48] Devos O, Gabrielli C, Tlili MM, Tribollet B. Nucleation-Growth process of scale electrodeposition: Influence of the supersaturation. Electrochem. Soc. 2003;**150**:494-501

[49] Ben Amor M, Zgolli D, Tlili MM, Manzola SA. Influence of water hardness, substrate nature and temperature on heterogeneous calcium carbonate nucleation. Desalination. 2004;**166**:79-84. DOI: 10.1016/j. desal.2004.06.061

[50] Karoui H, Korchef A, Tlili MM, Mosrati H, Gil O, Mosrati R, et al. Effects of Mg^{2+}, Ca^{2+} and SO_4^{2-} ions on precipitation kinetics and microstructure of aragonite. Ann. Chim. Sci. Mater. 2008;**33**:123-134

[51] Fernández-Díaz L, Fernández-González Á, Prieto M. The role of sulfate groups in controlling $CaCO_3$ polymorphism. Geochim. Cosmochim. Acta. 2010;**74**:6064-6076. DOI: 10.1016/ j.gca.2010.08.010

[52] Liu X, Li K, Wu C, Li Z, Wu B, Duan X, et al. Influence of copper (II) on biomineralization of CaCO3 and preparation of micron pearl-like biomimetic CaCO3. Ceram. Int. 2019; **45**:14354-14359. DOI: 10.1016/j. ceramint.2019.04.150

[53] Mucci A, Morse JW. The incorporation of Mg^{2+} and Sr^{2+} into calcite overgrowths. Influence of growth rate and solution composition. Geochim. Cosmochim Acta. 1983;**4**:

7217-7233. DOI: 0016-7037/83/ 020217-17503.00/0

[54] Busenberg E, Plummer LN. Kinetic and thermodynamic factors controlling the distribution of SO_4^{2-} and Na^+ in calcites and selected aragonites. Geochim. Cosmochim. Acta. 1985;**49**: 713-725. DOI: 10.1016/0016-7037(85) 90166-8

[55] Hu Z, Deng Y. Supersaturation control in aragonite synthesis using sparingly soluble calcium sulfate as reactants. J. Colloid Interf. Sci. 2003; **266**:359-365. DOI: 10.1016/S0021-9797 (03)00699-4

[56] Chen T, Neville A, Yuan M. Influence of Mg2+ on CaCO3 formation-bulk precipitation and surface deposition. Chem. Eng. Sci. 2006;**61**: 5318-−5327. DOI: 10.1016/j. ces.2006.04.007

[57] Vavouraki AI, Putnis CV, Putnis A, Koutsoukos PG. An atomic force microscopy study of the growth of calcite in the presence of sodium sulfate. Chem. Geol. 2008;**253**:243-251. DOI: 10.1016/j.chemgeo.2008.05.013

[58] Konrad F, Purgstaller B, Gallien F, Mavromatis V, Gane P, Dietzel M. Influence of aqueous Mg concentration on the transformation of amorphous calcium carbonate. J. Cryst. Growth. 2018;**498**:381-390. DOI: 10.1016/j. jcrysgro.2018.07.018

[59] Cuesta Mayorga I, Astilleros JM, Fernandez-Diaz L. Precipitation of $CaCO_3$ polymorphs from aqueous solutions: The role of pH and sulfate groups. Minerals. 2019;**9**:178. DOI: 10.3390/min9030178

[60] Ko M, Laycock NJ, Ingham B, Williams DE. In situ synchrotron X-ray diffraction studies of CO2 corrosion of carbon steel with scale inhibitors ATMPA and PEI at 80°C. Corros. 2012; **68**:1085-1093. DOI: 10.5006/0657

[61] Hamdouni A, Montes-Hernandez G, Tlili MM, Findling N, Renard F, Putnis CV. Removal of Fe(II) from groundwater via aqueous portlandite carbonation and calcite-solution interactions. Chem. Eng. J. 2016;**283**: 404-411. DOI: 10.5006/0657

[62] Korchef A, Kerkeni I, Ben Amor M, Galland S, Persin F. Iron removal from aqueous solution by oxidation, precipitation and ultrafiltration. Desalin. Water Treat. 2009;**9**:1-8. DOI: 10.5004/dwt.2009.745

[63] EU. Drinking Water Directive; Council Directive 98/83/EC of 3 November 1998. Official Journal of the European Communities L330/32 from 5.12.1998. Available at: http://eurlex. europa.eu/LexUriServ/site/en/oj/1998/ l_330/l_33019981205en00320054.pdf

[64] Tlili MM, Ben Amor M, Gabrielli C, Joiret S, Maurin G, Rousseau P. Study of electrochemical deposition of $CaCO_3$ by in situ raman spectroscopy: II. Influence of the solution composition. J. Electrochem. Soc. 2006;**150**:485-493

[65] Tlili MM, Ben Amor M, Gabrielli C, Joiret S, Maurin G. On the initial stages of calcium carbonate precipitation. Eur. J. Water Qual. 2006;**37**:89-108

[66] Paquette J, Vali H, Mucci A. TEM study of Pt-C replicas of calcite overgrowths precipitated from electrolyte solutions. Geochim. Cosmochim. Acta. 1996;**60**:4689-4701. DOI: 10.1016/S0016-7037(96)00270-0

[67] Morse WJ, Arvidson RS, Luttge A. Calcium carbonate formation and dissolution. Chem. Rev. 2007;**107**: 342-381. DOI: 10.1021/cr050358j

[68] Rushdi AI, Pytkowicz RM, Suess E, Chen CT. The effect of magnesium-to-calcium ratios in artificial seawater at different ionic products, upon the induction time and mineralogy of calcium carbonate: A laboratory study. Geol. Rdsch. 1992;**81**:751-758

[69] Reddy MM. Effect of magnesium ion on calcium carbonate nucleation and crystal growth in dilute aqueous solutions at 25° celsius, studies in diageneses, U.S. Geological survey, Denver, Bulletin. 1986; 1578:169–182.

[70] Chen T, Neville A, Yuan M. Assessing the effect of Mg^{2+} on $CaCO_3$ scale formation–bulk precipitation and surface deposition. J. Cryst. Growth. 2005;**275**:1341-1347. DOI: 10.1016/j. jcrysgro.2004.11.169

[71] Kelland MA. Effect of various cations on the formation of calcium carbonate and barium sulphate scale with and without scale inhibitors. Ind. Eng. Chem. Res. 2011;**50**:5852-5861. DOI: 10.1021/ie2003494

[72] Di Lorenzo F, Burgos-Cara A, Ruiz-Agudo E, Putnis CV, Prieto M. Effect of ferrous iron on the nucleation and growth of $CaCO_3$ in slightly basic aqueous solutions. CrystEngComm. 2017;**19**: 447-460. DOI: 10.1039/c6ce02290a

[73] Herzog RE, Shi Q, Patil JN, Katz JL. Magnetic water treatment: The effect of iron on calcium carbonate nucleation and growth. Langmuir. 1989;**5**:861-867. DOI: 10.1021/la00087a048

[74] Katz JL, Reik MR, Herzog RE, Parsiegla KI. Calcite growth inhibition by iron. Langmuir. 1993;**9**:1423-1430. DOI: 10.1021/la00029a043

[75] Pernot B, Euvrard M, Simon P. Effect of iron and manganese on the scaling potentiality of *water*. J. Water SRT – Aqua. 1998;**47**:21-29. DOI: 10.2166/aqua.1998.0004

[76] Takasaki S, Parsiegla KI, Katz JL. Calcite growth and the inhibitory effect of iron(III). J. Cryst. Growth. 1994;**143**: 261-268. DOI: 10.1016/0022-0248(94) 90066-3

[77] Macadam J, Parsons SA. Calcium carbonate scale and control, effect of material and inhibitors. Water Sci. Technol. 2004;**49**:153-159. DOI: 10.2166/wst.2004.0112

[78] Ruiz-Agudo E, Putnis CV, Rodrigues-Navarro C, Putnis A. Effect of pH on calcite growth at constant aCa^{2+}/aCO_3^{2-} ratio and supersaturation. Geochim. Cosmochim. Acta. 2011;**75**: 284-296. DOI: 10.1016/j. gca.2010.09.034

[79] Elgqulst B, Wedborg M. Stability of ion pairs from gypsum solubility, degree of ion pair formation between the major constituents. Mar. Chem. 1975;**3**:215-225. DOI: 10.1016/0304-4203(75)90003-1

[80] Sucha L, Cadek J, Hrabek K, Vesely J. The stability of the chloro complexes of magnesium and of the alkaline earth metals at elevated temperature. Collect. Czech. Chem. Commun. 1975;**40**:2020-2024. DOI: 10.1135/cccc19752020

[81] Johnson KS, Pytkowicz RM. Ion association with H+, Na+, K+, Ca2+, and Mg2+ in aqueous solutions at 25 degrees C. Am. J. Sci. 1978;**278**:1428-1447. DOI: 10.2475/ajs.278.10.1428

[82] Majer V, Stulik K. A study of the stability of alkaline earth metal complexes with fluoride and chloride ions at various temperatures by potentiometry with ion selective electrodes. Talanta. 1982;**29**:145-148. DOI: 10.1016/0039-9140(82)80039-8

[83] Allakhverdov GR. Calculation of the formation constants of singly charged complex ions of bivalent metals in solution. Russ. J. Phys. Chem. 1985;**59**: 39-41

[84] Williams-Jones AE, Seward TM. The stability of calcium chloride ion pairs in aqueous solutions at temperatures between 100 and 360°C. Geochim. Cosmochim. Acta. 1989;**53**:

313-318. DOI: 10.1016/0016-7037(89) 90383-9

[85] Takita Y, Eto M, Sugihara H, Nagaoka K. Promotion mechanism of co-existing NaCl in the synthesis of $CaCO_3$. Mater. Lett. 2007;**61**:3083-3085. DOI: 10.1016/j.matlet.2006.11.005

[86] Ukrainczyk M, Gredicak M, Jeric I, Kralj D. Interactions of salicylic acid derivatives with calcite crystals. J. Colloid Interface Sci. 2012;**365**:296-307. DOI: 10.1016/j.jcis.2011.09.009

[87] Natsi PD, Rokidi SG, Koutsoukos PG. Precipitation of calcium carbonate ($CaCO_3$) in water-monoethylene glycol solutions. Ind. Eng. Chem. Res. 2019;**58**:4732-4743. DOI: 10.1021/acs.iecr.8b04180

[88] Oral CM, Kapusuz D, Ercan B. Enhanced vaterite and aragonite crystallization at controlled ethylene glycol concentrations. Sakarya Univ. J. Sci. 2019;**23**:129−138. DOI: 10.16984/ saufenbilder.433985

[89] Zhang D, Lin Q, Xue N, Zhu P, Wang Z, Wang W, et al. The kinetics, thermodynamics and mineral crystallography of $CaCO_3$ precipitation by dissolved organic matter and salinity. Sci. Total Environ. 2019;**673**:546-552. DOI: 10.1016/j.scitotenv.2019.04.138

[90] Džakula BN, Fermani S, Dubinsky Z, Goffredo S, Falini G, Kralj D. In vitro coral biomineralization under relevant aragonite supersaturation conditions. Chem. Eur. J. 2019;**25**:10616-10624. DOI: 10.1002/ chem.201900691

[91] Ostwald W. Lehrbuch für allgemeine Chemie, Vol II, Engelman, Leipzig, 1902.

[92] Bamford CH, Tipper CFH. Comprehensive Chemical Kinetics, Vol. 22, Reactions in the Solid State, Elsevier, Amsterdam, 1980.

[93] Cardew PT, Davey RJ, Ruddick AJ. Kinetics of polymorphic solid-state transformations. J. Chem. Soc., Faraday Trans. 2. 1984;**80**:659-668. DOI: 10.1039/F29848000659

[94] Davey RJ, Ruddick AJ, Guy PD, Mitchell B, Maginn SJ, Polywka LA. The IV-III polymorphic phase transition in ammonium nitrate: A unique example of solvent mediation. J. Phys., D: Appl. Phys. 1991;**24**:176-185

[95] Kralj D, Brečević L, Kontrec J. Vaterite growth and dissolution in aqueous solution III. Kinetics of transformation. J. Cryst. Growt. 1997; **177**:248-257. DOI: 10.1016/S0022-0248 (96)01128-1

[96] Han YS, Hadiko G, Fuji M, Takahashi M. Influence of initial CaCl2 concentration on the phase and morphology of $CaCO_3$ prepared by carbonation. J. Mater. Sci. 2006;(14): 4663-4667. DOI: 10.1007/s10853-006-0037-4

[97] Kitano Y, Okumura M, Idogaki M. Incorporation of sodium, chloride and sulfate with calcium carbonate. Geochem Journal. 1975;**9**:75-84. DOI: 10.2343/geochemj.9.75

[98] Menadakis M, Maroulis G, Koutsoukos PG. Incorporation of Mg^{2+}, Sr^{2+}, Ba^{2+} and Zn^{2+} into aragonite and comparison with calcite. J. Math. Chem. 2009;**46**:484-491. DOI: 10.1007/ s10910-008-9490-4

[99] Lahann RW. A chemical model for calcite crystal growth and morphology control. J. Sediment. Petrol. 1978;**48**: 337-344. DOI: 10.1306/212F746E-2B24-11D7-8648000102C1865D

[100] Folk RL. The natural history of crystalline calcium carbonate: effect of magnesium content and salinity. J. Sediment. Petrol. 1974;**44**:40-35. DOI: 10.1306/74D72973-2B21-11D7-8648000102C1865D

[101] Chave KE, Deffeyes KS, Weyl PK, Garrels RM, Thompson ME. Observations on the solubility of skeletal carbonates in aqueous solutions. Science. 1962;**137**:33-34. DOI: 10.1126/ science.137.3523.33

[102] Kontrec J, Kralj D, Brečević L, Falini G, Fermani S, Noethig-Laslo V, et al. Incorporation of inorganic anions in calcite. Eur. J. Inorg. Chem. 2004; (23):4579-4585. DOI: 10.1002/ ejic.200400268

[103] Strand S, Hognesen EJ, Ausad T. Wettability alteration of carbonates— Effects of potential determining ions (Ca^{2+} and SO_4^{2-}) and temperature. Colloids Surf. A: Physicochem. Eng. Aspects. 2006;**275**:1-10. DOI: 10.1016/j. colsurfa.2005.10.061

[104] Koetzee PP, Yacoby M, Howall S, Mubenga S. Scale reduction and scale modification effect induced by Zn and other metal species in physical water treatment. Water SA. 1998;**24**:77-84

[105] Mejri W, Ben Salah I, Tlili MM. Speciation of Fe(II) and Fe(III) effect on CaCO3 crystallization. Cryst. Res. Technol. 2015;**50**:236-243. DOI: 10.1002/crat.201400444

[106] Esmaeely SN, Choi YS, Young D, Nesic S. Effect of Calcium on the formation and protectiveness of iron carbonate layer in CO_2 corrosion. Corrosion. 2013;**69**:912-920. DOI: 10.5006/0942

[107] Alsaiari HA, Kan A, Tomson M. Effect of calcium and iron (II) ions on the precipitation of calcium carbonate and ferrous carbonate. Soc. Petrol. Eng. J. 2010;**15**:294-300. DOI: 10.2118/ 121553-PA

[108] Mansoori H, Young D, Brown B, Nesic S, Singer M. Effect of CaCO3-saturated solution on CO_2 corrosion of mild steel explored in a system with controlled water chemistry and well-

defined mass transfer conditions. Corros. Sci. 2019;**158**:108078. DOI: 10.1016/j.corsci.2019.07.004

[109] Morgan B, Lahav O. The effect of pH on the kinetics of spontaneous Fe(II) oxidation by O_2 in aqueous solution-basic principles and a simple heuristic description. Chemosphere. 2007;**68**: 2080-2084. DOI: 10.1016/j. chemosphere.2007.02.015

[110] Wang T, Colfen H, Antonietti M. Nonclassical crystallization: Mesocrystals and morphology change of $CaCO_3$ crystals in the presence of a polyelectrolyte additive. J. Am. Chem. Soc. 2005;**127**:3246-3247. DOI: 10.1021/ ja045331g

[111] Rizzo R, Gupta S, Rogowska M, Ambat R. Corrosion of carbon steel under CO2 conditions: Effect of $CaCO_3$ on the stability of the $FeCO_3$ protective layer. Corros. Sci. 2019;**162**:108214. DOI: 10.1016/j.corsci.2019.108214

[112] Pernot B, Euvrard M, Remy F, Simon P. Influence of Zn(II) on the crystallisation of calcium carbonate application to scaling mechanisms. J. Water Serv. Res. Technol. Aqua. 1999; **48**:16-23

[113] Al-Hamzah AA, East CP, Doherty WOS, Fellows CM. Inhibition of homogenous formation of calcium carbonate by poly (acrylic acid). The effect of molar mass and end-group functionality. Desalination. 2014;**338**: 93-105. DOI: 10.1016/j. desal.2014.01.020

[114] Li X, Gao B, Yue Q, Ma D, Rong H, Zhao P, et al. Effect of six kinds of scale inhibitors on calcium carbonate precipitation in high salinity wastewater at high temperatures. J. Environ. Sci. 2015;**29**:124-130. DOI: 10.1016/j. jes.2014.09.027

[115] Xu Z, Zhao Y, Wang J, Chang H. Inhibition of calcium carbonate fouling on heat transfer surface using sodium carboxymethyl cellulose. Appl. Therm. Eng. 2019;**148**:1074-1080. DOI: 10.1016/j.applthermaleng.2018.11.088

[116] Zuo Z, Yang W, Zhang K, Chen Y, Li M, Zuo Y, et al. Effect of scale inhibitors on the structure and morphology of $CaCO_3$ crystal electrochemically deposited on TA1 alloy. J. Colloid Interf. Sci. 2020;**562**: 558-566. DOI: 10.1016/j.jcis.2019.11.078

[117] Yu W, Wang Y, Li A, Yang H. Evaluation of the structural morphology of starch- graft -poly(acrylic acid) on its scale-inhibition efficiency. Water Res. 2018;**141**:86-95. DOI: 10.1016/j. watres.2018.04.021